Structural and dynamical properties of ionic liquids: a molecular dynamics study employing DL_POLY 4

Qamreen Parker[a,b], Robert G. Bell[a] and Nora H. de Leeuw [a,b]

[a]Department of Chemistry, University College London, London, UK; [b]School of Chemistry, Cardiff University, Cardiff, UK

ABSTRACT

Molecular dynamics simulations are often used to study the structures and dynamics of ionic liquids. Here, we have simulated three ionic liquids, trihexyl(tetradecyl)-phosphonium chloride [P_{66614}][Cl], 1-butyl-3-methylimidazolium acecate [BMIm][Oac] and 1-ethyl-3-methylimidazolium dicyanamide, [EMIm][DCA] in a comparison of two force fields, GAFF and CL&PFF. In most cases, the resulting theoretical densities agree with experimental values within a 2% error. Diffusive properties were characterised by mean squared displacements to show the significant effect of the alkyl chain on the movement of the [P_{66614}] cation. Activation energies of diffusion were calculated from linear Arrhenius plots which agree with previous studies. Simulations of the dynamical behaviour show retention of short and medium-range structure of the ionic liquids with temperature. However, although with increasing temperature more high energy local configurations become accessible, they are observed less frequently as energy barriers are more easily overcome, resulting in more ordered time-averaged structures.

KEYWORDS

Ionic liquids; molecular dynamics simulations; phosphonium-based cations

1. Introduction

Ionic liquids (ILs) are salts, which are liquid at ambient and near-ambient (<100°C) temperatures and usually contain bulky organic groups, either on the cation/anion or both. Due to the inability of these bulky ions to close-pack, the cohe-sive energy is remarkably low, making these organic salts compounds with low melting temperatures. ILs can be made up of a variety of ions with functional groups, which can change the physical and chemical properties of the IL, e.g. the viscosity, density, or adsorptive behaviour. The highly tuneable properties of ionic liquids are advantageous for many applications, including in gas separation, electrolytes and catalytic solvents [1–3]. Some general attributes of ILs are negligible vapour pressure, high thermal stability, non-flammability, ability to act as polar solvents and high ionic conductivity [4]. These properties have over the last 30 years resulted in significant interest from the academic and industrial communities, generating a substantial fundamental and applied research literature on these environmentally friendly materials.

The properties of ILs make them suitable for use in selective gas absorption, including the capture of carbon dioxide, where the sorption of gas molecules can be tailored by understanding and tuning the properties of the IL. For example, density and viscosity are key attributes that need to be understood, considered and successfully predicted for a range of ILs. Molecular simulations can elucidate the basic physical chemistry of ILs, e.g. how the structures and compositions of ILs relate to the physical properties exhibited. Systematic studies into the behaviour and properties of ILs can be carried out using a var-iety of computational techniques, such as Monte Carlo and molecular dynamics (MD) simulations [5–7]. Here, we have used MD simulations to investigate the structures and properties of a number of prominent IL systems.

Choosing a suitable and reliable force field is important to the validity and accuracy of the IL simulations. To this end, the first section of this paper details the comparison of two force fields widely used to simulated ILs: Generalised AMBER force field (GAFF) and Canongia Lopez and Padua force field (CL&PFF). GAFF was developed to simulate large organic and biological molecules [8] and as the ions considered in this study are all of a bulky organic nature, GAFF is a good force field to consider. CL&PFF is a IL-specific force field that has been parameterised for various IL ions [9]. As we aim to explore a variety of ions that are representative of cur-rent IL research, three different ILs are considered: trihexyl(tet-radecyl)-phosphonium chloride, [P_{66614}][Cl] (melting point: −50°C); 1-butyl-3-methylimidazolium acecate, [BMIm][Oac] (melting point: >30°C); and 1-ethyl-3-methylimidazolium dicyanamide, [EMIm][DCA] (melting point: −21°C)[10]. The IL constituent ions and their structures are shown in Table 1. We aim to compare these systems in terms of density and IL structure, showing any similarities and differences obtained from the two force fields.

Phosphonium cation-based ILs are easily synthesised [7,8], and may offer superior properties, such as high thermal stability [11], when compared to the more well-researched nitrogen cation-based ILs, e.g. imidazolium and pyrrolidinium cations [11]. Work into phosphonium-based salts developed later than nitrogen-based ILs, owing to tributylphosphonium only becoming available on a large scale after 1990, followed by the availability of tetrabutylphosphonium chloride and bromide on a multi-ton scale [9]. Variations of the four

Table 1. Names, structural formulae and abbreviations of the cations and anions used in this study.

Name	Formula	Abbreviation
1-Butyl-3-methylimidazolium	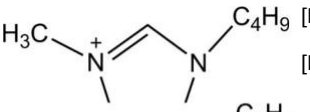	$[BMIm]^+$
1-Ethyl-3-methylimidazolium	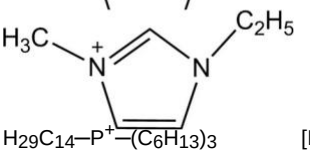	$[EMIm]^+$
Trihexyl (tetradecyl)phosphonium	$H_{29}C_{14}–P^+–(C_6H_{13})_3$	$[P_{66614}]^+$
Acetate	$(H_3C)COO^-$	$[Oac]^-$
Bis (trifluoromethanesulfonyl)imide	$N^-(SO_2CF_3)_2$	$[NTf_2]^-$
Chloride	Cl^-	$[Cl]^-$
Acetate	$(H_3C)COO^-$	$[Oac]^-$
Dicyanamide	$N^-(CN)_2$	$[DCA]^-$

substituents on the phosphonium cation and the paired anion provide for a large range of different IL salts. A number of experimental studies have been carried out on the structure and properties of the phosphonium-based IL trihexyl(tetradecyl)-phosphonium bis(trifluoromethanesulfonyl)imide, $[P_{66614}][NTf_2]$ (melting point: −72.4°C) [9,10]. In contrast, whilst simulation studies have been carried out [12], in-depth computational work is less readily available. For example, Liu et al. have reported a comparison of an all-atom FF with a united-atom FF, which showed not unexpectedly that the all-atom FF yielded better agreement of liquid density with experimental data, before calculating heat capacities [13]. In this work, we have also studied the ionic liquid $[P_{66614}][NTf_2]$ to obtain a detailed description of its structure and diffusive properties at different temperatures.

2. Computational methods

2.1. Force field comparison and validation

A standard 'class I' force field of the form in Equation (1) was used to represent the atomic interactions in the IL. It contains harmonic bonding and angle-bending terms, as well as 4-body terms where appropriate for intramolecular interactions, and electrostatic and Lennard-Jones terms to describe the intermolecular non-bonded interactions. The $[P_{66614}][Cl]$ LJ potential parameters for both force fields used in this work are listed in Table 2.

$$U(r) = \sum_{\text{bonds}} \frac{1}{2} k_b (r - r_0)^2 + \sum_{\text{angles}} \frac{1}{2} k_u (u - u_0)^2 + \sum_{\text{dihedrals}} k_F [1 + \cos(mF - d_0)] \quad (1)$$

Table 2. Lennard Jones parameters used for $[P_{66614}][Cl]$, σ in Å and ε in kJ mol^{-1}, for both CL&PFF and GAFF [8,14].

	CL&PFF		GAFF	
Atom	σ	ε	σ	ε
P	3.74	0.837	3.74	0.837
C	3.50	0.276	3.40	0.360
H	2.50	0.125	2.65	0.063
Cl	3.65	0.830	3.47	1.109

Table 3. Ionic liquids simulated along with the number of ion pairs for each simulation box.

Ionic liquid	Number of ion pairs
$[P_{66614}][Cl]$	250
[BMIm][Oac]	797
[EMIm][DCA]	1062

PACKMOL [15] was used to build initial systems of similar numbers of atoms ~25500 to keep the system sizes comparable (Number of ion pairs in Table 3). AMBER 12 [16] and DL_POLY 4 [17] were used for minimisations and MD calculations using the GAFF and CL&P force fields, respectively. PACKMOL avoids the creation of high-energy local configurations by guaranteeing that short-range repulsive interactions are avoided. Additionally, systems are extensively equilibrated before the production runs. At a single temperature, different PACKMOL starting configurations were generated and, following equilibration, these were found to yield systems of near identical structural properties.

In order to achieve the correct density, the isothermal-isobaric (NPT) ensemble was employed, using the Berendsen thermostat and barostat set at 298 K and 1 atm. A time step of 1 fs was used for a total production run of a 5 ns trajectory. If a system was unstable and initial simulations failed, the canonical ensemble (NVT) was used and slow heating starting at 5 K was performed. An equilibration was considered successful only after stable and consistent results (energy and density) over periods of at least 500 ps. Simple cubic periodic boundaries were used for all simulations.

The reason two different MD programs were used for the two different force fields was simply due to the ease of setting up the simulations with these force fields, and for comparison of calculation time and performance. AMBER, a package of molecular simulation programs used widely in biochemistry [18], is primarily used to model relatively large organic molecules and biological compounds. DL_POLY 4 was compared to DL_POLY Classic [19] to explore the balance between system size and calculation time, where we found that for our systems DL_POLY 4 was computationally faster than Classic running on a reduced number of compute cores.

2.2. Trihexyl(tetradecyl)-phosphonium bis (trifluoromethanesulfonyl)imide $[P_{66614}][NTf_2]$

$$
+ \sum_{\text{improper dihedrals}} \frac{1}{2} k_{\Phi} (\Phi - \Phi_0)^2
$$

$$
+ \sum_{i} \sum_{j=i}^{\text{non-bonded interactions}} 4\epsilon_{ij} \left[\left(\frac{\sigma_{ij}}{r_{ij}} \right)^{12} - \left(\frac{\sigma_{ij}}{r_{ij}} \right)^{6} \right] + \frac{1}{4\pi\epsilon_0} \frac{q_i q_j}{r_{ij}} \quad (1)
$$

Liquid-phase classical molecular dynamics (MD) simulations were performed of trihexyl(tetradecyl)-phosphonium bis(trifl-uoromethanesulfonyl)imide, $[P_{66614}][NTf_2]$, using the DL_POLY 4 program package. The initial configurations for ... pairs in a large simulation cell using the PACKMOL program.

The dispersion interactions were evaluated using a cut-off of 10 Å, and the smoothed particle mesh Ewald (SPME) method was used to treat the full electrostatic interactions. The trajectories were integrated using the velocity Verlet algorithm with a time step of 1 fs. The temperature and pressure were controlled by the Berendsen method with relaxation times of 0.8 and 1 ps, respectively. Ionic liquid force field parameters were taken from the CL&P force field which has been used widely in previous work and is validated for three different ILs in the first section of this study. To minimise possible high energy structures in the initial configuration, a short 200 ps minimisation run was carried out of a low-density system, followed by a simulation at 500 K and 500 atm for 500 ps, to reduce the volume of the box. This combination was employed as it offered the optimal balance for the systems between speed of equilibration and accuracy of the densities, as compared with experiment. The NPT ensemble was employed, and the density was calculated over a 5 ns MD trajectory, after a 2 ns equilibration run at temperatures of 298, 323, 348, 373 and 398 K. The liquid struc-ture and mean squared displacement of the ions were calcu-lated from a 5 ns production run. Radial and spatial distribution functions were calculated from the trajectories using TRAVIS ('TRajectory Analyzer and VISualizer') [20].

3. Results and discussion

3.1. Force field comparison and validation

First, three well-characterised ionic liquids were used to vali-date the methodology before expanding the simulations to a less well-studied system. The primary property of the simulated systems that can be compared easily to experimental data is density. Experimental densities [21] are well reproduced by molecular dynamics calculations with both force fields (see Table 4). CL&PFF achieves values closer to experiment, redu-cing the percentage differences by a factor of >2 compared to GAFF. It is evident that both force fields reproduce the exper-imental densities much better for the imidazolium-based ILs, which could be due to the significantly different structures of the phosphonium-based versus the imidazolium-based ionic liquid, with the former possessing much greater confor-mational flexibility. Accurately modelling a substantial number of large organic molecules made up of long alkyl chains poses an additional challenge compared to rigid imidazolium aro-matic units with short side chains [18,19].

As seen above, the densities derived from the MD calcu-lations using both force fields are generally in good agreement with experimental data and thus neither can be discounted using this data comparison alone. Next, site-site radial distri-bution functions (RDFs) of ionic liquid [P_{66614}][Cl] were calcu-lated at 298 K, shown in Figure 1. RDFs are often used to describe any long-range order in liquid and amorphous materials, and these were calculated to characterise differences in the structures resulting from the different force fields.

Table 4. Densities, at 298 K, of ionic liquids simulated compared to experimental data with percentage differences (%). Experimental data from Zhang et al. [21].

Density/mol dm^{-3}	[P_{66614}][Cl] (%)	[BMIm][Oac] (%)	[EMIm][DCA] (%)
Experimental	1.698	5.321	6.258
CL&PFF	1.660 (−1.8)	5.316 (−0.1)	6.262(+0.06)
GAFF	1.630 (−4.1)	5.294 (−0.5)	6.279(+0.3)

The phosphorus-to-phosphorus, P-P, RDF (see Figure 1 (top)) for both FFs shows a peak centred on 7 Å with a first minimum at 10 Å, indicating a large solvation shell. A differ-ence between the FFs is the small shoulder at 5 Å seen with CL&P, which is much less pronounced in the GAFF curve. A more defined long-range order is seen with CL&P (black line), i.e. a second shell centred around 14 Å and a third shell at 20 Å. The tetrahedral geometry around the phosphorus atom, with long alkyl chains in every direction, means that the approach of another phosphorus within a 5 Å radius is not possible.

The first peak in the chloride-to-chloride, Cl-Cl, RDF (Figure 1(centre)) at 7.5 Å is again well-defined for both force fields, with more defined long range order observed with CL&PFF, which is comparable to previous MD simu-lations by Maginn [22] and by Padua et al. [23].

The cation–anion interactions are in good agreement between the two FFs. In Figure 1(bottom), a large peak at ~4 Å is seen with a g(r) of 15.5 for CL&PFF and 12.0 for GAFF. The first solvation shell finishes at 7 Å, then a second peak centred around 10 Å. Coordination numbers for the cation–anion corresponding to the first shell in the g(r) are calculated from n(r) plots, also shown in Figure 1, to be 2.5 and 2.4 for CL&PFF and GAFF, respectively. Any long-range order is insignificant, but CL&PFF again shows more defined order beyond 10 Å. The g(r) values of the cation–anion interaction, characterised by the height of the first peak, is at least a factor of 4 greater than the interactions of ions of like charge.

3.2. Density and diffusive behaviour of [P_{66614}][NTf_2]

Having compared the two force fields by carrying out MD simulations on the three known ILs above, we noted that the CL&PFF produced a closer match to experimental densities and more defined structural features. The RDFs calculated from the MD simulations with CL&PP show a typical liquid structure with a well-defined first peak and broader peaks at longer range, which however were much less distinct in the GAFF RDF analysis. Our next study on the lesser known [P_{66614}][NTf_2] ionic liquid system was therefore carried out solely with the CL&PFF force field and the DL_POLY 4 code.

The agreement between the simulated density obtained from the CL&PFF simulations at a temperature of 298 K, i.e. 1.409 mol dm^{-3}, and the experimental density of 1.394 mol dm^{-3} is very good, with a discrepancy of only 1%. The slight over-estimation in density of simulated ionic liquids systems is also seen in other studies [22,24,25]. Liu et al. [12], compar-ing an all-atom force field and a united-atom force field in mol-ecular dynamics simulations of phosphonium-based ionic liquids, found that the united atom force field over-estimated the density even further compared to experimental densities at 293 K.

3.1.1. Mean squared displacements in [P_{66614}][NTf_2]

The CL&PFF force field uses different atom types within the cation and anion (Figure 2). Translational dynamics were quantified via mean square displacements (MSDs), which

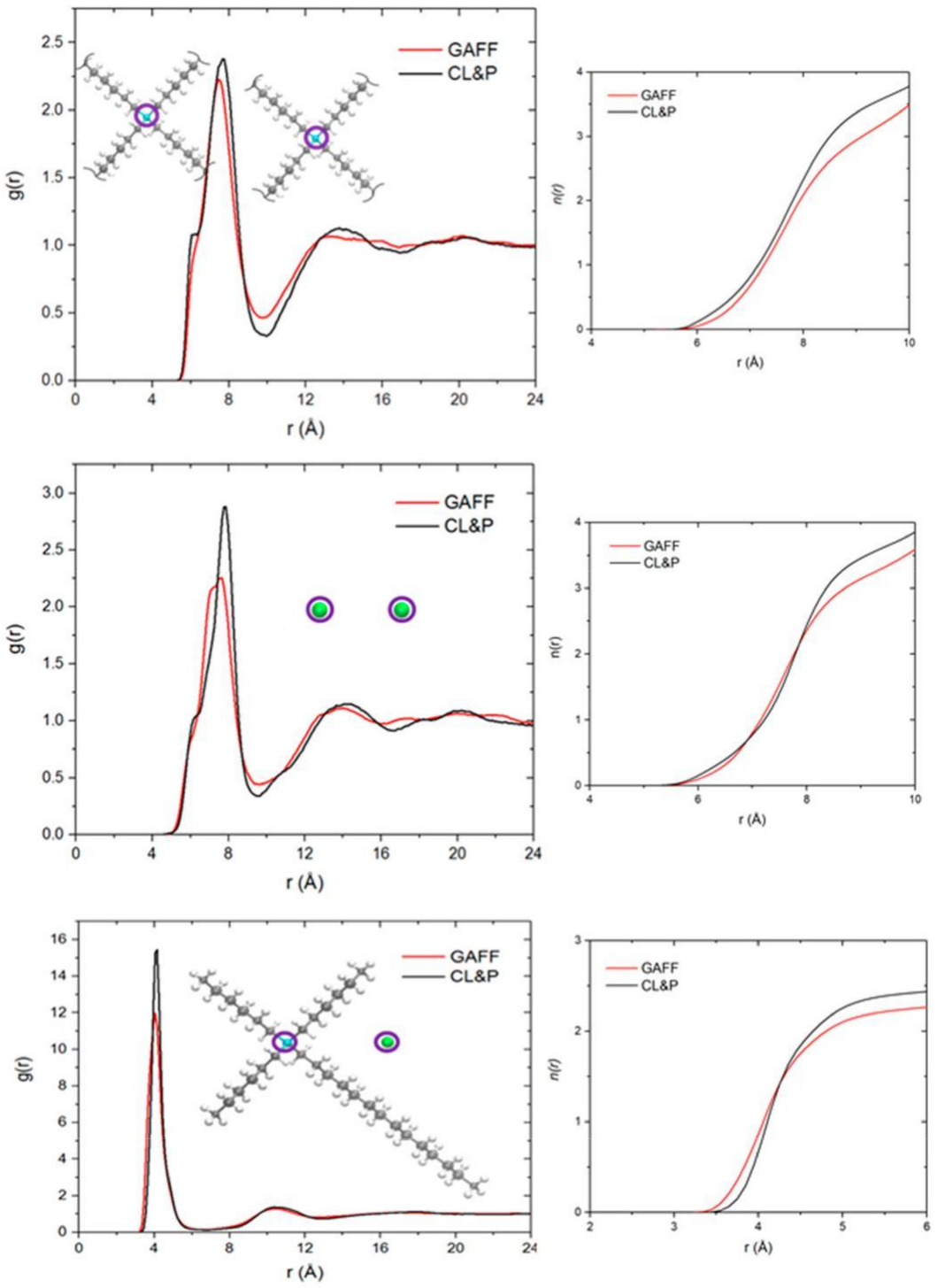

Figure 1. (Colour online) Site-site radial distribution function g(r) vs distance, r (Å), at T = 298 K, for [P_{66614}][Cl]. Cation-P to cation-P (top), anion Cl^- to Cl^- (middle) and cation-P to anion-Cl^- (bottom). n(r) plots for the first coordination shell are displayed to the right of each RDF.

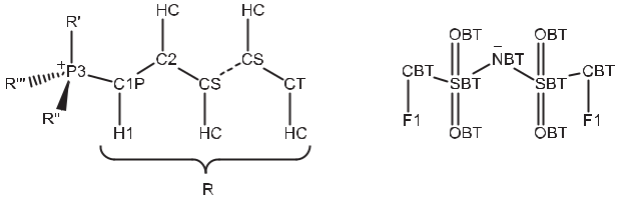

Figure 2. Adopted nomenclature for atom types in tetra-alkyl phosphonium cation, [P_{66614}] and bis(trifluoromethanesulfonyl)imide anion, [NTf_2].

were calculated for each of the independently moving atom types at the five simulated temperatures (Figures 3 and 4). Different atom types are considered explicitly to reveal greater detail of the movement of the ions, rather than using single centre-of-mass MSDs. The HC atoms are considered to follow so closely the movement of the carbon atoms to which they are bonded, that we did not consider that separate MSDs for the HC atoms would provide additional insight. The P3 and NBT atoms are the central and most highly charged atoms of

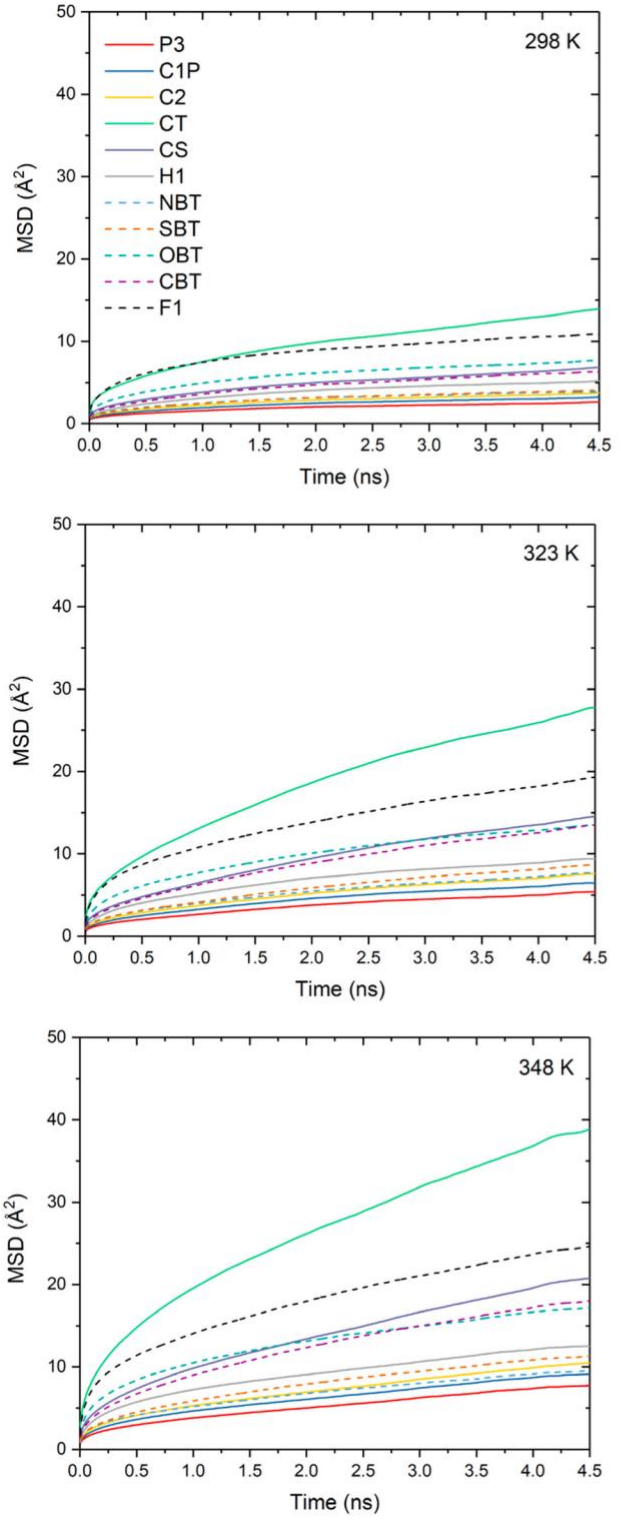

Figure 3. (Colour online) Mean square displacement of each atom type in the [P_{66614}][NTf_2] system, at temperatures 298, 323 and 348 K.

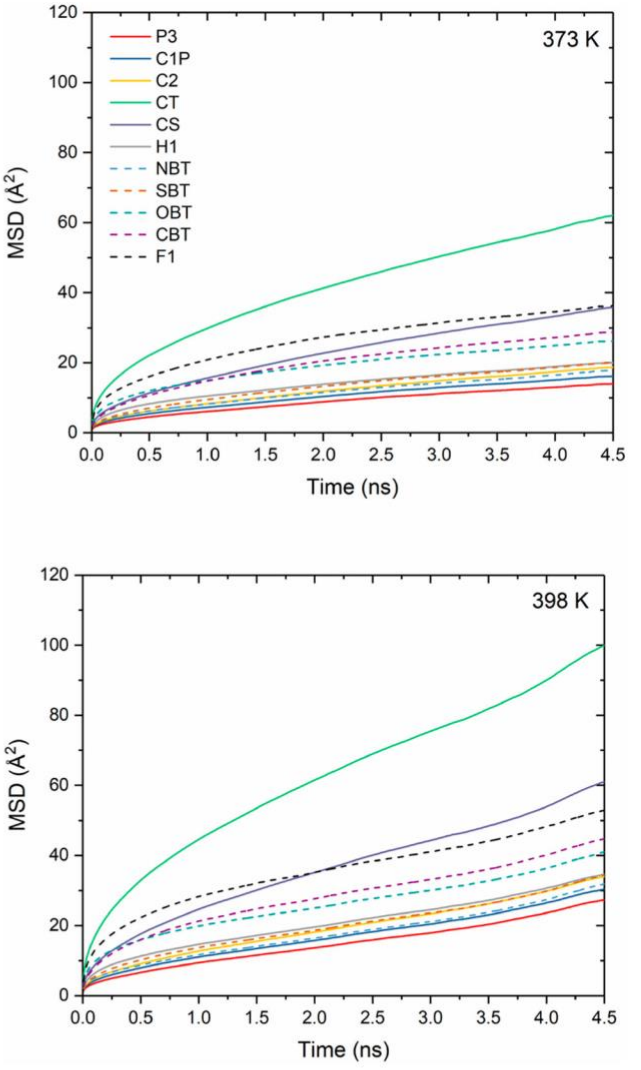

Figure 4. (Colour online) Mean square displacement of each atom type in the [P_{66614}][NTf_2] system, at temperatures 373 and 398 K.

the IL and are considered the key atoms of the cation and anion, respectively. We note a greater range of diffusivity in the cation atom types compared to the anion, which can be attributed to the difference in size between the two ions as well as the long-hydrocarbon chain nature of the cation.

To quantify the movement of the cation and anion as entire species, the individual atom type MSDs are summed with respect to their contribution to the ion, i.e. there is a single P3 in every cation, but 4 C1P and 4 CT so the latter are multiplied by 4. Finally, to estimate the movement of the ionic liquid, all atom types are combined by a weighted average method for the MSD of the ion pair (IP). The MSDs of the cation, anion and IP are shown in Figure 5.

The self-diffusion coefficients of the atom types in the ionic liquid (Table 5) were calculated from the MSDs of the atom types (Figures 3–5). The slopes of the MSDs are plotted between 0.25 and 4.5 ns and the gradients are divided by 6 as per the MSD equation for a 3-dimensional simulation:

$$\langle r^2 \rangle = 6Dt \quad (2)$$

Ionic liquids tend to have slow dynamics and the range of our calculated self-diffusion coefficients agree with values from the literature [26,27].

The diffusivity of the anion is greater than the cation, D_{NTf2} = 1.45 × 10^{-12} m^2 s^{-1} cf. D_{P66614} = 1.33 × 10^{-12} m^2 s^{-1} at 298 K, because the anion is significantly smaller, has no long alkyl chains and occupies a smaller volume. It therefore experiences less steric hindrance and is able to move more easily. However,

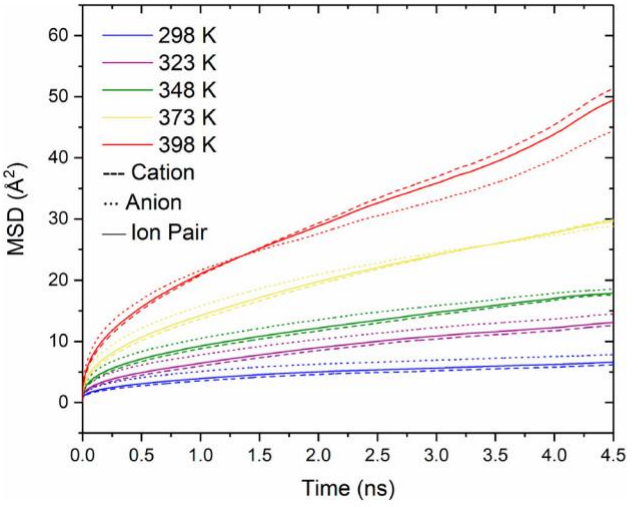

Figure 5. (Colour online) Mean square displacement of entire cation (dashed lines), anion (dotted lines) and averaged for total ion pair (solid lines) in [P66614-][NTf2], at temperatures 298 K (blue), 323 K (purple), 348 K (green), 373 K (yellow) and 398 K (red).

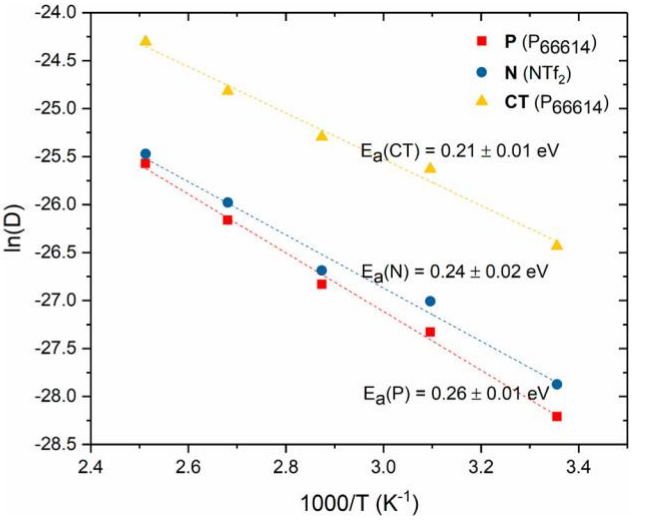

Figure 6. (Colour online) Arrhenius plots of diffusion coefficients of phosphorus (P) and terminal carbons (CT) of cation [P66614] and nitrogen (N) of anion [NTf2].

Table 5. Diffusion coefficients, × 10^{-12} m^2 s^{-1}, of phosphonium atom (P) and terminal carbons (CT) of the cation, [P66614], the nitrogen atom (N) of the anion, [NTf2], the entire cation, the entire anion and the average for the ionic pair, [P66614][NTf2].

Temperature /K	P	N	CT	[P_{66614}^+]	[NTf_2^-]	IP
298	1.44	2.05	6.83	1.33	1.45	1.37
323	1.55	2.16	7.67	3.32	3.00	3.00
348	2.23	2.57	10.33	4.52	4.22	4.45
373	4.35	5.22	16.67	8.05	6.67	7.68
398	7.84	8.68	27.83	14.37	10.75	13.38

as the temperature increases, there is a notable jump in the diffusion coefficient of the cation compared to the anion. We suggest that this increase in diffusion of the cation with temperature may be due to the greater flexibility of its alkyl chains as the temperature is increased.

3.1.2. Activation energies of diffusion

Arrhenius plots for the diffusion of key atom types in [P66614-][NTf2] are shown in Figure 6, with the derived activation energies displayed on the plots. The activation energies are all in the range of 0.20–0.26 eV, which agrees with literature values for the activation energies of diffusion of ionic liquids. For example, Heintz et al. reported activation energies of imidazolium ILs in the range of 0.18–0.20 eV [28].

In order to compare the diffusion behaviour with temperature for the cation versus the anion, relevant Arrhenius plots are shown in Figure 7, including the activation energies of diffusion. We calculated E_a(P66614) to be 0.24 eV, whilst E_a(NTf2) is 0.20 eV. Although the difference is small, the lower value for the [NTf2] anion is consistent with it being more mobile than the [P66614] cation, as evidenced by its higher diffu-sion coefficient.

3.1.3. Intramolecular spatial distribution functions

Further into the cation's dynamic behaviour at different temperatures can be achieved by utilising spatial distribution functions (SDFs) of the terminal carbons of the alkyl chains

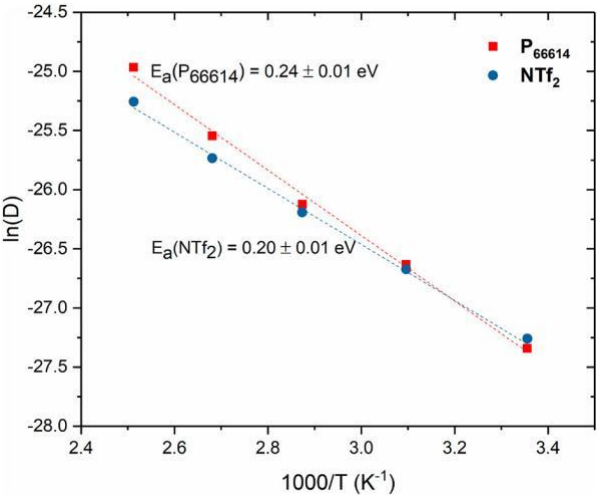

Figure 7. (Colour online) Arrhenius plots of diffusion coefficients of cation [P66614] and anion [NTf2].

relative to the phosphorus central atom, as shown in Figure 8. Assuming that the statistics obtained are sufficient, the rougher iso-surface at the lowest temperature of 298 K indicates more restricted movement of the terminal carbon on the timescale of the simulation. Conversely, as the temperature increases, we observe enhanced relative motion of the alkyl chains, as shown by the smoothed, more regular iso-surface. As already mentioned, this enhanced mobility of the alkyl chains may well contribute to the increased MSD of the cation with temperature.

3.2. Effect of temperature on structure of [P66614][NTf2]

The effect of temperature on the structure of the IL is considered in Figure 9, showing the RDFs for (a) phosphorus of cation to nitrogen in anion, P–N, (b) phosphorus of cation to cation, P–P, and (c) nitrogen of anion to anion, N–N. The

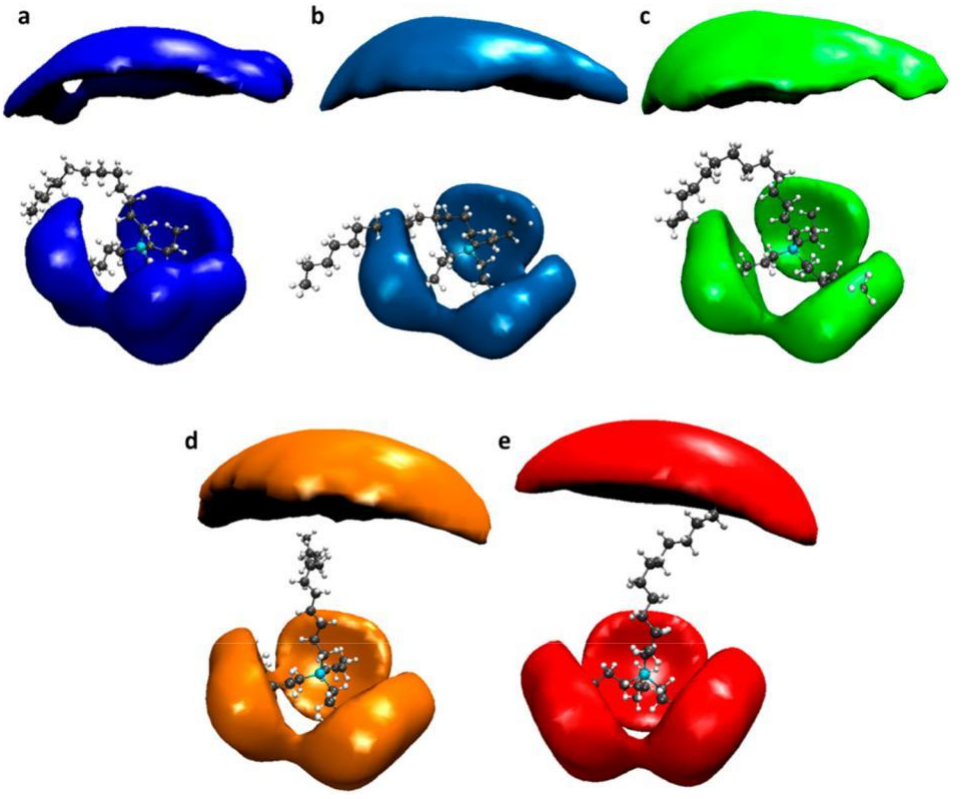

Figure 8. (Colour online) Intramolecular spatial distribution functions (SDFs) of the 4 terminal carbons (CT) around the central phosphorus atom in $[P_{66614}][NTf_2]$, at 5 different temperatures: (a) 298 K, (b) 323 K, (c) 348 K, (d) 373 K and (e) 398 K. Isovalue of 0.25 is used, with the reference molecule created from the first time step.

like-ion to ion RDFs show long-range order in the IL structure, with anion–anion interactions occurring at a closer approach than cation–cation, due to the difference in sizes of the two ions; the anion is significantly smaller, whilst the cation is bulk-ier and globular.

We observe that the first solvation shell sharpens with increasing temperature for all three RDFs. It appears that at 298 K, there is more structure with shoulders in both like-like ion RDFs (Figure 9(b,c)). With increasing temperature, however, the local minima coalesce, resulting in a smoother RDF and higher intensity coordination peaks for all three shells. This temperature effect is most distinct in the P-P interaction (Figure 9(b)).

3.2.1. Cis/Trans behaviour of NTf_2

The ratio of the cis/trans orientation of the bis(trifluoromethanesulfonyl)imide anion, $[NTf_2]$, can be obtained from the simulation in two ways. The first is the distribution of $CF_3\cdots CF_3$ distance and the second is the distribution of the C–S···S–C torsional bond angle, as seen in Figure 10. A clear bimodal distribution is seen in both the $CF_3\cdots CF_3$ distances and the C–S···S–C torsional bond angles. The cis configuration corresponds to the $CF_3\cdots CF_3$ distance of ~4.2 Å and the C–S···S–C torsional bond angle of ~40°, and the trans configuration corresponds to the $CF_3\cdots CF_3$ distance of ~5.1 Å and the C–S···S–C torsional bond angle of ~170°. At 298 K, about 80% of the anions in the simulation exist in the trans configuration. These findings are comparable to previous experimental and computational studies of 1,3-dimethylimidazolium bis(trifluoromethylsulfo-nyl)imide, [29] and other $[NTf_2]$-based ionic liquids [30].

The effect of increasing the temperature of the system from 298 to 323 K seems to have no significant effect on the cis-trans ratio of the $[NTf_2]$. However, at 348, 373 and 398 K we see even fewer cis conformations as the ratio moves further to the trans conformation. A possible reason for this change could be a balance between thermodynamic and kinetic factors. Although we could expect a larger proportion of the higher energy cis conformers to be present at higher temperatures, upon heating, it will also become easier to overcome the cis-to-trans energy barrier, which will be lower from trans to cis, than from cis to trans. Depending on the relative energies between the conformers and the cis-to-trans energy barriers, over time we could expect a decrease in the probability of finding the higher energy cis configuration relative to the lowest energy trans configuration.

4. Conclusions

Molecular dynamics simulations of ionic liquids are a growing field and a viable option to explore and elucidate the structures and interactions within ionic liquids. Experimental densities are well reproduced with force field methods, as seen in this work and by the previous literature cited in this study. Both force fields considered here, CL&PFF and GAFF, marginally underestimate the densities of the ionic liquids, with CL&PFF achieving densities closer to experimental data. Some simi-larities are seen in the structures produced for all the ILs

$[P_{66614}][Cl]$ and [BMIm][Oac] with the different force fields (i.e. RDF first shells), but greater long range order is observed with CL&PFF, possibly due to the greater ionicity of the parameterisation. The density of the [EMIm][DCA] only is

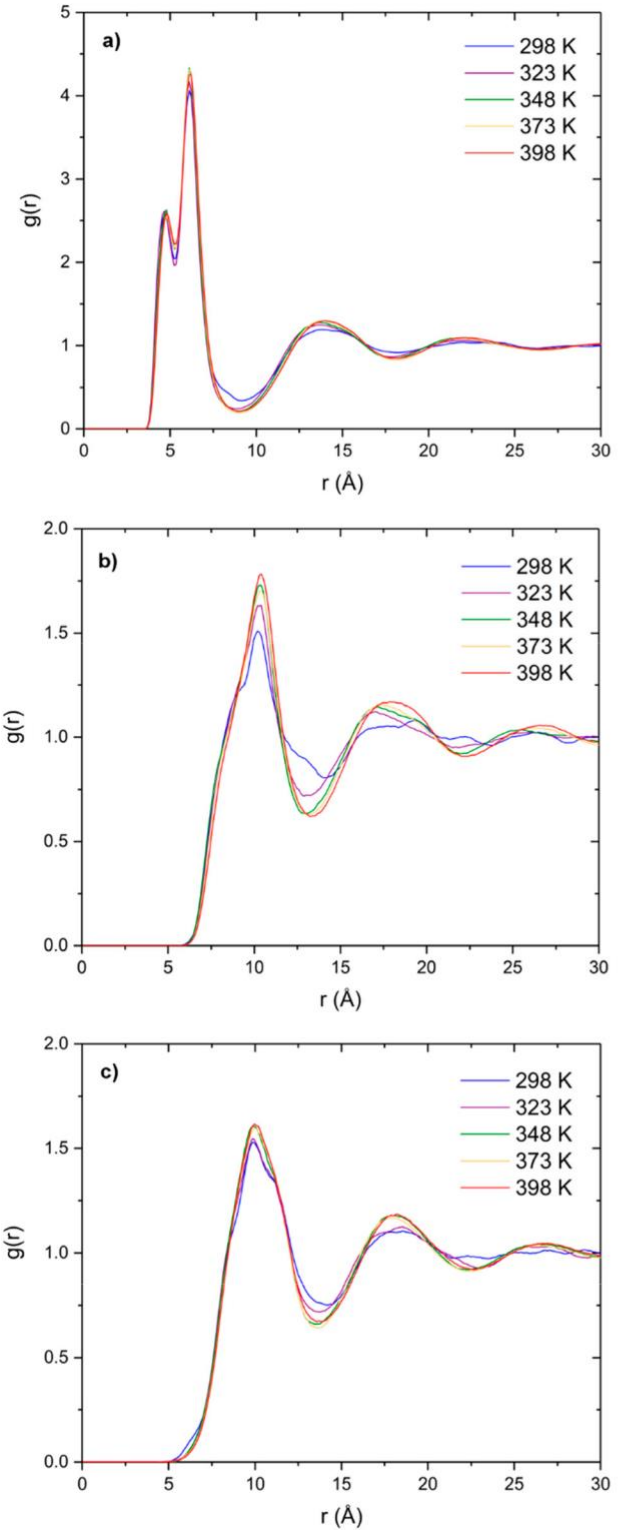

Figure 9. (Colour online) Site-site intermolecular radial distribution functions in $[P_{66614}][NTf_2]$ ionic liquid at increasing temperatures: (a) RDF of phosphorus atom of P^{+}_{66614} to nitrogen atom of $[NTf_2]$ (cation to anion), (b) P to itself of P_{66614} (cation to cation) and (c) N to itself (anion to anion).

overestimated by both force fields, which may be due to the underestimation of atom charges in the DCA ion.

After successfully modelling the density, we have used the CL&PFF to evaluate the diffusion of different atom types in the IL $[P_{66614}][NTf_2]$, along with the average for the cation, anion and the ion pair. We conclude that the cation diffuses

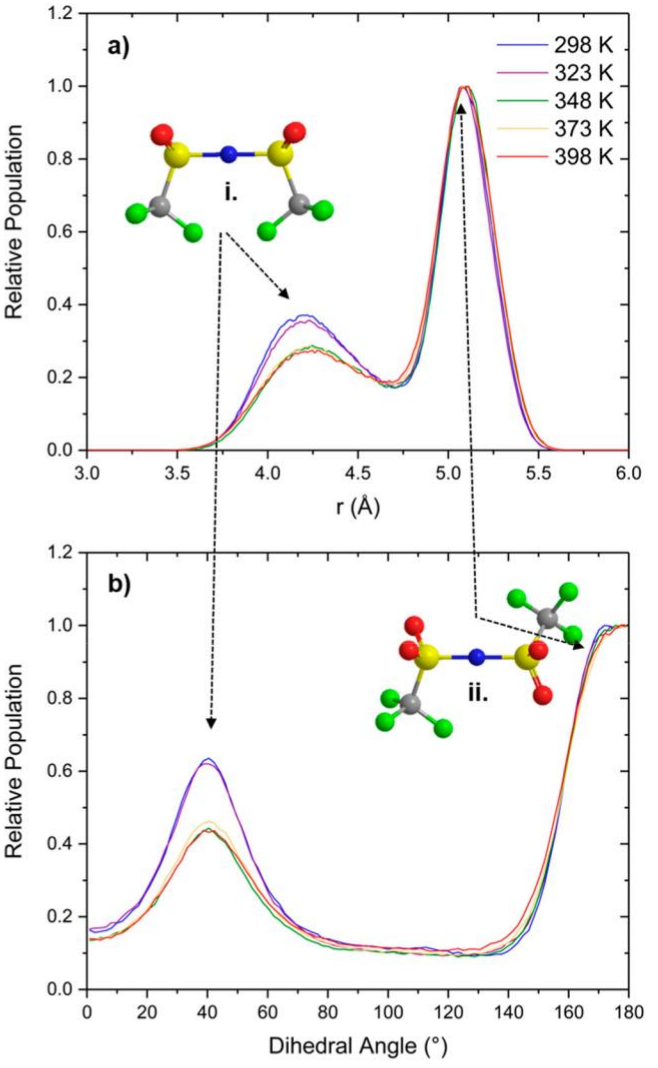

Figure 10. (Colour online) Distribution of the (a) $CF_3\cdots CF_3$ distances and (b) C–S···S–C dihedral angle as a function of the number of anions in liquid $[P_{66614}][NTf_2]$, at different temperatures. Models showing (i) the cis and (ii) the trans configuration of the bis(trifluoromethanesulfonyl)imide anion, $[NTf_2]$.

more slowly than the anion, and that the trend in diffusivity of the simulated system is comparable to experimental viscos-ities of ILs [31]. The structure of the ionic liquid is investigated through RDFs and compared across different temperatures to demonstrate significant structural changes. Finally, when heat-ing the IL, the cis/trans configuration ratio in the anion $[NTf_2]$ indicates that a qualitative structural change occurs between 323 and 348 K, which can be linked to the apparent sharpening of the RDF peaks on increasing the temperature. An expla-nation for this trend is that the simulated structure, at higher temperatures, is spending less time in local energy minima as the activation energies to move into the lowest energy configur-ation can be overcome more easily.

The work reported in this study illustrates the application of molecular dynamics simulations in investigations of the struc-tural and dynamical properties of ionic liquids. We further demonstrate that force fields, based on standard potential func-tions, can reproduce the experimental densities and provide atomic-level information on the long-range structures of these complex systems that are difficult to obtain from

experiment. Future work will include predictive MD simulations of the uptake of carbon dioxide in the IL systems.

Acknowledgements

Finally, the authors also acknowledge the use of the UCL@Legion and UCL@Grace High Performance Computing Facility, and associated support services, in the completion of this work.

Disclosure statement

No potential conflict of interest was reported by the authors.

Funding

This work was carried out as part of the '4CU' programme grant, aimed at the sustainable conversion of carbon dioxide into fuels, led by the Univer-sity of Sheffield and carried out in collaboration with the University of Manchester, Queen's University Belfast, University College London and Cardiff University. The authors therefore gratefully acknowledge the Engineering and Physical Sciences Research Council (EPSRC) for support-ing this work financially [grant number EP/K001329/1]. Via our member-ship of the UK's HPC Materials Chemistry Consortium, which is funded by EPSRC [EP/L000202], this work made use of the facilities of ARCHER, the UK's national high-performance computing service, which is funded by the Office of Science and Technology through EPSRC's High End Com-puting Programme.

ORCID

Nora H. de Leeuw http://orcid.org/0000-0002-8271-0545

References

[1] Wilkes JS. A short history of ionic liquids-from molten salts to neo-teric solvents. Green Chem. 2002;4(2):73–80. DOI:10.1039/B110838G

[2] Wei D, Ivaska A. Applications of ionic liquids in electrochemical sensors. Anal Chim Acta. 2008;607(2):126–135.

[3] Brennecke JF, Maginn EJ. Ionic liquids: innovative fluids for chemi-cal processing. AIChE J. 2001;47(11):2384–2389.

[4] Blanchard LA, Hancu D, Beckman EJ, et al. Green processing using ionic liquids and CO_2. Nature. 1999;399(6731):28–29. DOI:10.1038/ 19887

[5] Lee SH, Rasaiah JC. Molecular dynamics simulation of ion mobility. 2. Alkali metal and halide ions using the SPC/E model for water at 25 degrees C. J Phys Chem. 1996;100(4):1420–1425.

[6] Shah JK, Brennecke JF, Maginn EJ. Thermodynamic properties of the ionic liquid 1-n-butyl-3-methylimidazolium hexafluorophosphate from Monte Carlo simulations. Green Chem. 2002;4(2):112–118. DOI:10.1039/B110725A

[7] Shimizu K, Pensado A, Malfreyt P, et al. 2D or not 2D: structural and charge ordering at the solid-liquid interface of the 1-(2-hydro-xyethyl)-3-methylimidazolium tetrafluoroborate ionic liquid. Faraday Discuss. 2012;154(0):155–169. DOI:10.1039/C1FD00043H

[8] Wang J, Wolf RM, Caldwell JW, et al. Development and testing of a general amber force field. J Comput Chem. 2004;25(9):1157–1174. DOI:10.1002/jcc.20035

[9] Canongia Lopes J, Pádua AH. CL&P: a generic and systematic force field for ionic liquids modeling. Theor Chem Acc. 2012;131(3):1–11. DOI:10.1007/s00214-012-1129-7

[10] ChemFiles: enabling technologies ionic liquids, Vol. 5 No. 6. Available from: https://www.sigmaaldrich.com/content/dam/sigma-aldrich/docs/Aldrich/Brochure/al_chemfile_v5_n6.pdf

[11] Fraser K, MacFarlane DR. Phosphonium-based ionic liquids: an overview. Aust J Chem. 2009;62:309–321.

[12] Liu X, Zhou G, Zhang S, et al. Molecular simulations of phosphonium-based ionic liquid. Mol Simul. 2009;36(1):79–86. DOI:10. 1080/08927020903124569

[13] Ferreira AF, Simões PN, Ferreira AGM. Quaternary phosphonium-based ionic liquids: thermal stability and heat capacity of the liquid phase. J Chem Thermodyn [Internet]. 2012;45(1):16–27. Available from: http://www.sciencedirect.com/science/article/pii/S0021961411002953

[14] Canongia Lopes JN, Deschamps J, Pádua AAH. Modeling ionic liquids using a systematic all-atom force field. J Phys Chem B. 2004;108(6):2038–2047. DOI:10.1021/jp0362133

[15] Martínez L, Andrade R, Birgin EG, et al. PACKMOL: a package for building initial configurations for molecular dynamics simulations. J Comput Chem. 2009;30(13):2157–2164. DOI:10.1002/jcc.21224

[16] Case DA, Darden TA, Cheatham TE, et al. AMBER 12 [Internet]. San Francisco: University of California; 2012; Available from: http://ambermd.org/

[17] Todorov IT, Smith W, Trachenko K, et al. DL_POLY_3: new dimen-sions in molecular dynamics simulations via massive parallelism. J Mater Chem. 2006;16(20):1911–1918.

[18] Salomon-Ferrer R, Case DA, Walker RC. An overview of the amber biomolecular simulation package. Wiley Interdiscip Rev Comput Mol Sci. 2013;3(2):198–210. DOI:10.1002/wcms.1121

[19] Smith W, Forester TR. DL_POLY_2.0: a general-purpose parallel molecular dynamics simulation package. J Mol Graph. 1996;14(3):136–141.

[20] Brehm M, Kirchner B. TRAVIS – a free analyzer and visualizer for Monte Carlo and molecular dynamics trajectories. J Chem Inf Model. 2011;51(8):2007–2023. DOI:10.1021/ci200217w

[21] Zhang S, Sun N, He X, et al. Physical properties of ionic liquids: database and evaluation. J Phys Chem Ref Data. 2006;35(4):1475–1517. Available from: http://scitation.aip.org/content/aip/journal/jpcrd/35/4/10.1063/1.2204959

[22] Maginn EJ. Molecular simulation of ionic liquids: current status and future opportunities. J Phys Condens Matter [Internet]. 2009;21 (37):373101, Available from: http://stacks.iop.org/0953-8984/21/i= 37/a=373101.

[23] Canongia Lopes JNA, Pádua AAH. Nanostructural organization in ionic liquids. J Phys Chem B. 2006;110(7):3330–3335. DOI:10.1021/jp056006y

[24] Wendler K, Dommert F, Zhao YY, et al. Ionic liquids studied across different scales: a computational perspective. Faraday Discuss. 2012;154(0):111–132. DOI:10.1039/C1FD00051A

[25] Dommert F, Wendler K, Berger R, et al. Force fields for studying the structure and dynamics of ionic liquids: a critical review of recent developments. Chemphyschem. 2012;13(7):1625–1637. DOI:10. 1002/cphc.201100997

[26] Tsuzuki S, Shinoda W, Saito H, et al. Molecular dynamics simulations of ionic liquids: cation and anion dependence of self-diffusion coefficients of ions. J Phys Chem B. 2009;113(31):10641–10649. DOI:10.1021/jp811128b.

[27] Yue C, Fang D, Liu L, et al. Synthesis and application of task-specific ionic liquids used as catalysts and/or solvents in organic unit reactions. J Mol Liq [Internet]. 2011;163(3):99–121. Available from: http://www.sciencedirect.com/science/article/pii/S0167732211002923

[28] Heintz A, Lehmann JK, Schmidt E, et al. Diffusion coefficients of imidazolium based ionic liquids in Aqueous Solutions. J Solution Chem. 2009 Aug;38(8):1079–1083. DOI:10.1007/s10953-009-9431-2

[29] Deetlefs M, Hardacre C, Nieuwenhuyzen M, et al. Liquid structure of the ionic liquid 1,3-dimethylimidazolium Bis{(trifluoromethyl)sulfo-nyl}amide. J Phys Chem B. 2006;110(24):12055–12061. DOI:10. 1021/jp060924u

[30] Hanke K, Kaufmann M, Schwaab G, et al. Understanding the ionic liquid [NC4111][NTf2] from individual building blocks: an IR-spec-troscopic study. Phys Chem Chem Phys. 2015;17(13):8518–8529. DOI:10.1039/C5CP00116A

[31] Harris KR, Kanakubo M, Woolf LA. Temperature and pressure dependence of the viscosity of the ionic liquids 1-Hexyl-3-methylimidazolium Hexafluorophosphate and 1-butyl-3-methylimidazolium Bis(trifluoromethylsulfonyl)imide. J Chem Eng Data. 2007 May 1;52(3):1080–1085. DOI:10.1021/je700032n